Solid-State Diffusion Reaction and Formation of Intermetallic Compounds in the Nickel-Zirconium System

K. BHANUMURTHY, G.B. KALE, S.K. KHERA, and M.K. ASUNDI

Chemical diffusion studies in the nickel-zirconium system are investigated in the temperature range of 1046 to 1213 K employing diffusion couples of pure nickel and pure zirconium. Electron microprobe and X-ray diffraction studies have been employed to investigate the formation of different compounds and to study their layer growth kinetics in the diffusion zone. It is observed that growth of each phase is controlled by the process of volume diffusion as the layer growth obeys the parabolic law. The activation energies for interdiffusion in NiZr and NiZr$_2$, which are the dominant phases in the diffusion zone, are 119.0 ± 13.4 and 103.0 ± 25.0 kJ/mole, respectively. The formation and stability of compounds over the temperature range have been discussed on the basis of existing thermodynamic and kinetic data.

I. INTRODUCTION

THE formation of various intermetallics between two dissimilar metals has been a subject of great interest during the last two decades. The nickel-zirconium system finds its application in developing thermal barrier coatings on superalloys by a hot dipping process.[1] The latest nickel-zirconium phase diagram indicates eight intermetallic compounds (Figure 1), none of which exhibits extensive solubility.[2] The terminal solid solutions have very much restricted solid solubility. Three of the intermetallic compounds, namely, Ni$_7$Zr$_2$, NiZr, and NiZr$_2$, are congruently melting alloys, while four others, namely, Ni$_5$Zr, Ni$_{21}$Zr$_8$, Ni$_{10}$Zr$_7$, and Ni$_{11}$Zr$_9$, are formed by peritectic reaction. Ni$_3$Zr is also formed by peritectoid reaction. Recently, Hammad and Shaaban have reported interdiffusion studies in ZIRCALOY*-4 and pure nickel.[3]

*ZIRCALOY is a trademark of Westinghouse Electric Company, Pittsburgh, PA.

Thin-film studies on the formation of intermetallic compounds in the zirconium-nickel system have been reported.[4] The present paper deals with solid-state diffusion studies on bulk samples. Results on the formation of intermetallic compounds and the kinetics of layer growth in the temperature range of 1046 to 1213 K have been discussed. Stability of various intermetallic phases has been rationalized based on their diffusion behavior.

II. EXPERIMENTAL AND ANALYTICAL PROCEDURE

A. Preparation of Diffusion Couples

Rectangular pieces of pure zirconium (99.97 pct) and nickel (99.98 pct) approximately 10 × 5 × 3 mm in size

K. BHANUMURTHY, Scientific Officer, Metallurgy Division, G.B. KALE, Scientific Officer, Metallurgy Division, S.K. KHERA, Scientific Officer and Research Coordinator, Diffusion Research Group, Structural Metallurgy Section, Metallurgy Division, and M.K. ASUNDI, Head, Physical Metallurgy Division, are with the Bhabha Atomic Research Centre, Bombay 400085, India.
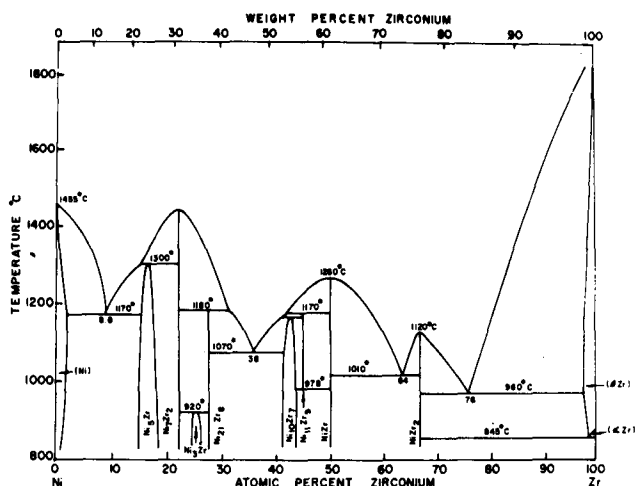Manuscript submitted September 15, 1989.

were cut from the rolled sheets. These specimens were encapsulated in silica tubes in helium atmosphere and annealed at 1173 K for 7 days for grain coarsening. The average grain size of zirconium was 1 to 2 mm and that of nickel was 0.5 to 1.0 mm. These specimens were metallographically polished to a 1-μm diamond finish. The polished faces of zirconium and nickel were kept in contact with each other and were loaded into a specially made jig under pressure in order to ensure intimate contact between two metal pieces. The entire assembly was placed in a vacuum furnace (vacuum better than 10^{-5} torr) for diffusion bonding at 1053 K for 15 minutes. Metallographic and microanalytical examination of the specimens indicated that the width of the diffusion zone prior to annealing treatment was negligible as compared to that obtained after diffusion annealing. The diffusion couples thus prepared were sealed under helium atmosphere and subsequently annealed in a preheated furnace controlling the temperature to within ±1 K in the temperature range of 1046 to 1213 K and for periods between 1 and 459 hours. Aluminum oxide powder was used for placing markers. Particles 0.1 to 1.0 μm in size were mixed with acetone, and a thin dilute layer was sprayed onto the freshly polished faces of nickel. These samples were dried, and diffusion couples were made as described above.

B. Optical Metallography

The annealed samples were mounted and polished perpendicular to the diffusion zone. The zirconium end of the diffusion couple was etched electrochemically, and the nickel end of the couple was chemically etched with a solution containing 20 pct HNO$_3$, 30 pct HCl, 20 pct H$_2$O$_2$, and 30 pct glycerol by volume.

C. Electron Probe Microanalysis

The marked areas of the diffusion couples were analyzed with the help of a Camebax electron probe microanalyzer operating at an accelerating voltage of 15 kV with a stabilized beam current of 100 nA. Both point counting and automatic line scans were employed to record the concentrations of zirconium and nickel. Lithium fluoride (LiF) and pentaerythritol (PET) crystals were

Fig. 1—Phase diagram of zirconium-nickel system.

used for dispersion of Ni K_α and Zr L_α lines, respectively. The raw intensity data thus obtained were corrected for atomic number, absorption, and fluorescence effects to get true concentration profiles.[5]

D. X-ray Diffraction Studies

The interfaces of the annealed samples were analyzed by a PHILIPS* X-ray diffractometer operating at 40 kV

*PHILIPS is a trademark of Philips Electronic Instruments Corporation, Mahwah, NJ.

and 20 mA. The diffractogram was recorded in the range of 2θ varying from 20 to 80 deg. The observed Bragg peaks were compared with the available ASTM data to identify the various intermetallic compounds.

E. Evaluation of Diffusion Coefficients

Boltzmann-Matano analysis[6] is generally employed to evaluate the interdiffusion coefficients in solid solution diffusion zones. By solving Fick's second law with the initial boundary conditions, $c = 0$ at $X < 0$ and $c = c_0$ at $X > 0$, the concentration-dependent interdiffusion coefficient is expressed as

$$\tilde{D}_{(c)} = -\frac{1}{2t}\frac{dX}{dc}\int_0^c X\,dc \qquad [1]$$

where t is the diffusion annealing time. The Matano interface, where $\int_0^{c_0} X\,dc = 0$, is taken as the origin of the x-axis. Heumann[7] has modified the above equation for cases where intermetallic compounds are observed in the diffusion zone. Assuming that phases I and III are coexisting with phase II, the diffusion coefficient for phase II can be given as

$$\tilde{D}_{(c)} = \frac{1}{2t}\cdot\frac{d}{[c_{II,I} - c_{II,III}]}\cdot\int_0^{c^{1/2}} X\,dc \qquad [2]$$

where $c_{II,I}$ and $c_{II,III}$ are the concentrations at the interface of phase II with I and that of phase II with III, respectively. The term $c^{1/2}$ is the mean of interface compositions, and d is the layer thickness of phase II.

Wagner's method[8] is more suitable to evaluate the interdiffusion coefficients for the line compounds. For a diffusion couple consisting of pure elements 1 and 2 and having very low solubility of the various intermediate phases, the interdiffusion coefficient $(\tilde{D}_i)$ for the phase i, coexisting with n number of phases, is expressed as

$$\int_{N_2^{i'}}^{N_2^{i''}} \tilde{D}_i\,dN_2 = (1 - N_2^i)\sum_{\nu=2}^{i-1}\frac{V_m^\nu N_2^\nu \Delta X^i \Delta X^\nu}{V_m^i(2t)}$$

$$+ \frac{N_2^i(1 - N_2^i)\,(\Delta X^i)^2}{2t}$$

$$+ N_2^i\sum_{\nu=i+1}^{n-1}\frac{V_m^\nu\cdot\{1 - N_2^\nu\}\cdot\Delta X^i\Delta X^\nu}{V_m^i\cdot 2t}$$

$$[3]$$

where ν is the serial number of the phase [$\nu = 1$ for the phase with the lowest mole fraction (N_2) of the component 2]. The terms V_m^i and ΔX^i are the molar volume and width of phase i, respectively. The terms $N_2^{i'}$ and $N_2^{i''}$ are the mole fraction of phase i coexisting with phases $i - 1$ and $i + 1$, respectively.

III. RESULTS AND DISCUSSION

A. Intermetallic Compounds and Layer Growth Kinetics

A typical photomicrograph of the diffusion zone of the couples annealed at 1133 K for 24 hours is shown in Figure 2. It can be seen clearly that five intermetallic compounds, namely, $NiZr_2$, $NiZr$, $Ni_{10}Zr_7$, Ni_7Zr_2, and Ni_5Zr, appear in the same order. It may be noted that a lot of porosity is observed on the nickel-rich side of the diffusion couple. The couple annealed at the higher temperature of 1213 K for 24 hours (Figure 3) shows only three compounds, namely, $NiZr_2$, $NiZr$, and Ni_5Zr. The phases Ni_7Zr_2 and $Ni_{10}Zr_7$ disappear at this temperature. The other three compounds, namely, Ni_3Zr, $Ni_{21}Zr_8$, and $Ni_{11}Zr_9$, do not form in the diffusion zone at all. The microstructure of the diffusion couple annealed at 1213 K for 144 hours is shown in Figure 4, and the microstructure of the NiZr compound is shown at higher magnification in Figure 5 (340 times) to reveal the grains clearly. It can be seen in both these photomicrographs that grains are randomly oriented in the diffusion zone, contrary to the observations in many systems.[9,10] A series of micrographs (Figures 6(a) through (c)) illustrate the formation of various compounds in the diffusion zone for the couples annealed at 1213 K for varying durations of time. These micrographs indicate systematic increase of the width of the diffusion zone with time. The X-ray diffraction peaks of these compounds have been compared with ASTM data to identify the compounds. The calculated d values (interplanar distances) for high intensity reflections match reasonably well. These results confirm the stoichiometry of the two dominant phases, namely, NiZr and $NiZr_2$.

The typical concentration penetration plots obtained by electron probe microanalysis (EPMA) for the couples annealed at 1213 K for 24 hours, 1133 K for 459 hours, and 1213 K for 144 hours are shown in Figures 7 through
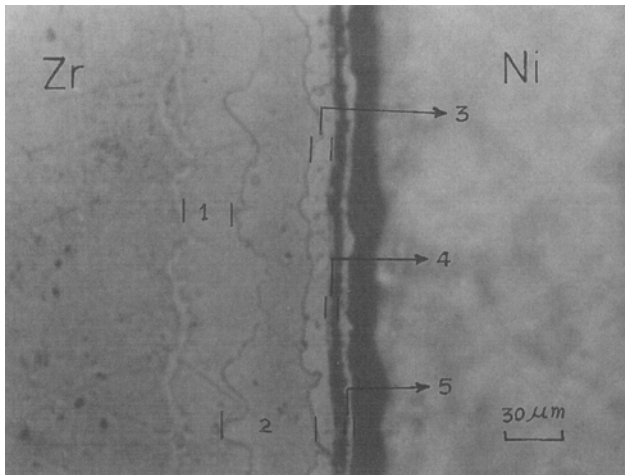
Fig. 2—Optical micrograph of the couple annealed at 1133 K for 24 h. The intermetallic compounds are marked as (1) $NiZr_2$, (2) NiZr, (3) $Ni_{10}Zr_7$, (4) Ni_7Zr_2, and (5) Ni_5Zr.
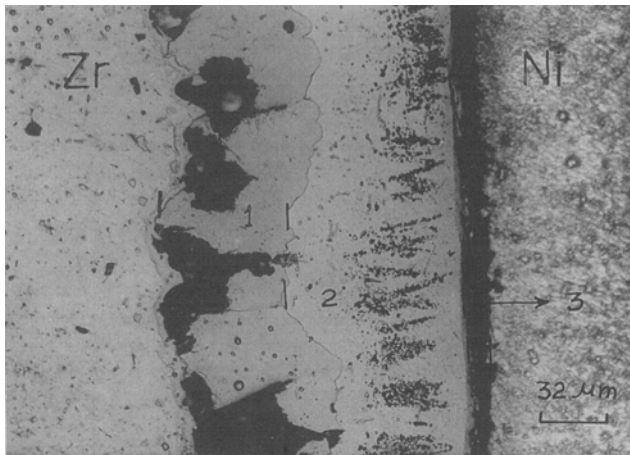

Fig. 3—Optical micrograph of the couple annealed at 1213 K for 24 h. The intermetallic compounds are marked as (1) $NiZr_2$, (2) NiZr, and (3) Ni_5Zr.
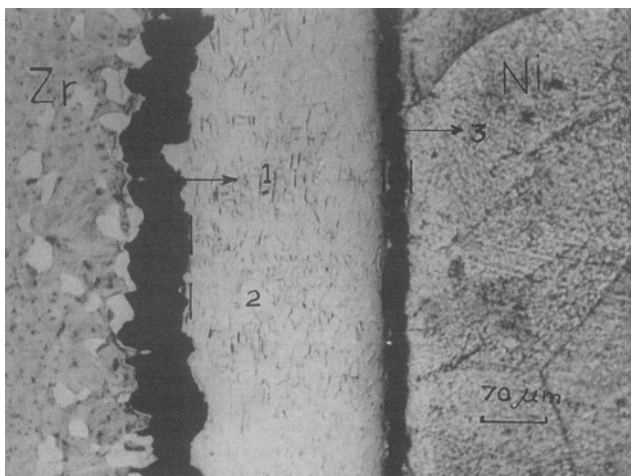

Fig. 4—Optical micrograph of the couple annealed at 1213 K for 144 h. The intermetallic compounds are marked as (1) $NiZr_2$, (2) NiZr, and (3) Ni_5Zr.
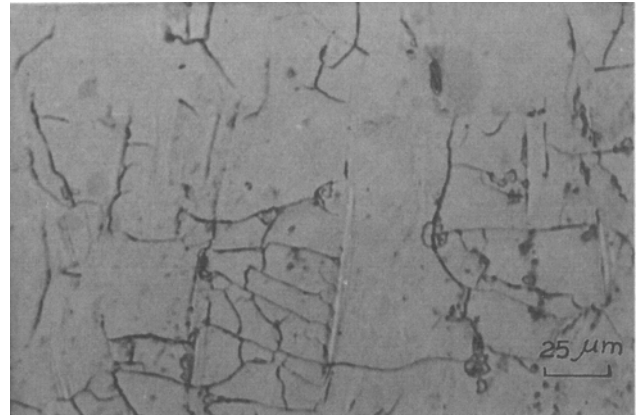

Fig. 5—Optical micrograph of the couple annealed at 1213 K for 144 h at higher magnification (340 times).

9, respectively. Various compounds observed and the corresponding widths as estimated by EPMA are listed in Table I. The time dependence of the growth of the diffusion zone can be expressed as

$$X = Kt^{1/n} \qquad [4]$$

where X is the phase thickness, K the reaction constant, t the time expressed in seconds, and n the reaction index.

The reaction constant, K, and index, n, have been evaluated from the intercept and the slope, respectively, using least mean square linear fit for log X vs log t plot. These values are listed in Table II. The reaction index is nearly equal to 2 for all of the compounds. The growth of all of the phases obeys the parabolic law, indicating that the growth is essentially through volume diffusion-controlled process. Small deviations in reaction index from the value of 2 have been reported by Castleman and Seigle[11] for a large number of systems. However, these deviations do not represent a change in diffusion mechanism. The backscattered electron image of the couple annealed at 1169 K for 24 hours' duration is shown in Figure 10. The presence of markers on the nickel-rich side indicates that the diffusion is controlled by vacancy mechanism and nickel diffuses more rapidly than zirconium. This observation has also been reported for thin-film zirconium/nickel couples.[12]
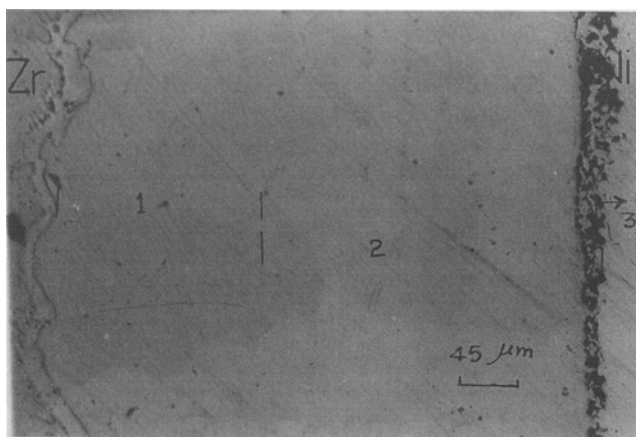
B. Composition of Intermetallic Compounds

The compositions of phase boundaries as reported in the zirconium-nickel phase diagram[2] and those estimated from the multiphase diffusion couples by spot analysis are listed in Table III. It can be seen that the compositions of various intermetallic compounds at the phase boundaries do not differ from those depicted by equilibrium phase diagram. Similar statistical indistinguishable compositions of coexisting phases in bulk as well as multiphase diffusion couples were reported.[13] Several workers[14-17] have discussed the consequences of nonattainment of local equilibrium on composition of phase boundaries. It is unlikely that matrix stresses, interfaces, and other nonequilibrium effects prevailing in
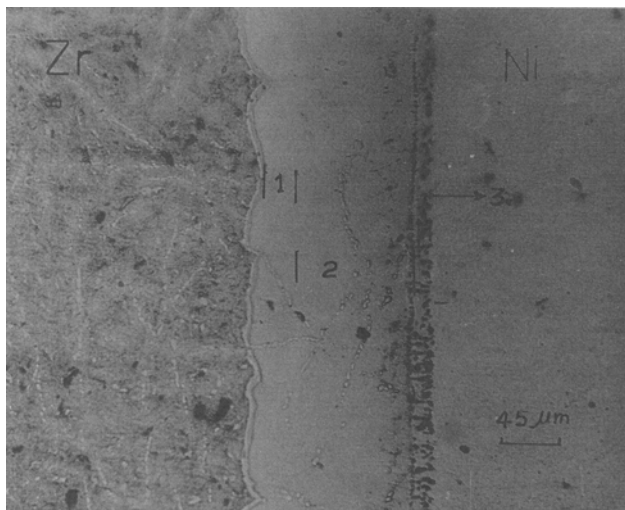
(a)
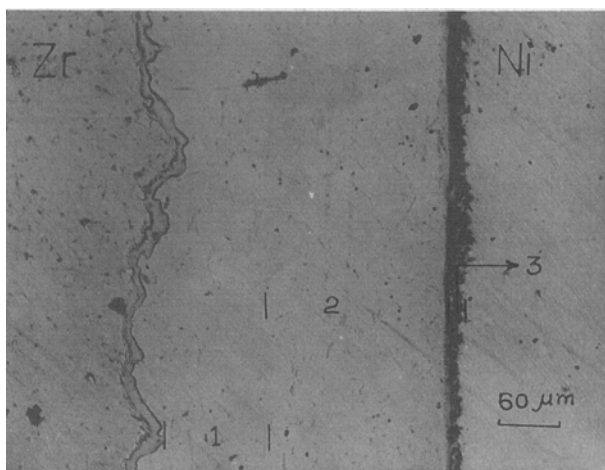
(b)

(c)

Fig. 6—Optical micrograph of the couple annealed at 1213 K for different durations: (a) 18 h (198 times), (b) 144 h (158 times), and (c) 334 h (174 times). The intermetallic compounds are marked as (1) NiZr₂, (2) NiZr, and (3) Ni₅Zr.

Fig. 7—Concentration penetration plots for the couple annealed at 1213 K for 24 h. The intermetallic compounds are marked as (1) NiZr₂, (2) NiZr, and (3) Ni₅Zr.

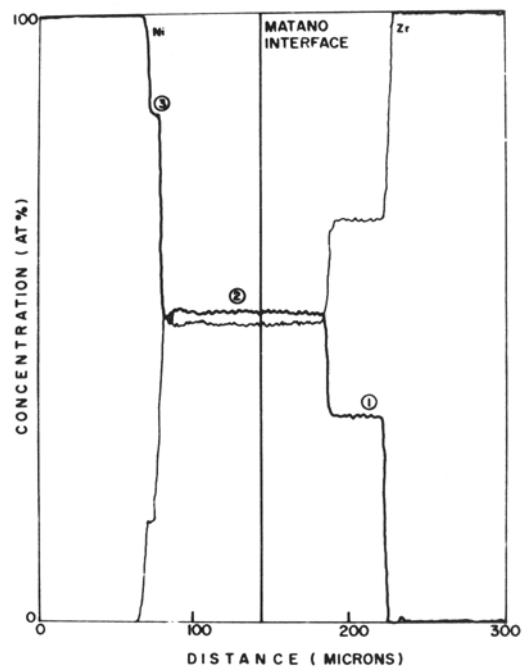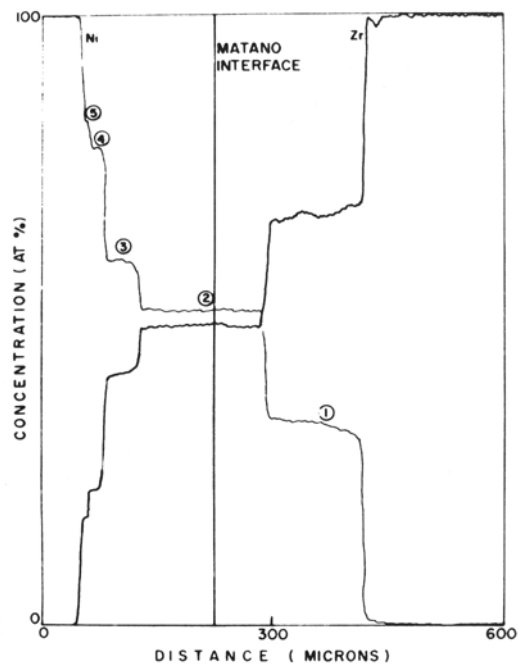
Fig. 8—Concentration penetration plots for the couple annealed at 1133 K for 459 h. The intermetallic compounds are marked as (1) NiZr₂, (2) NiZr, (3) Ni₁₀Zr₇, (4) Ni₇Zr₂, and (5) Ni₅Zr.
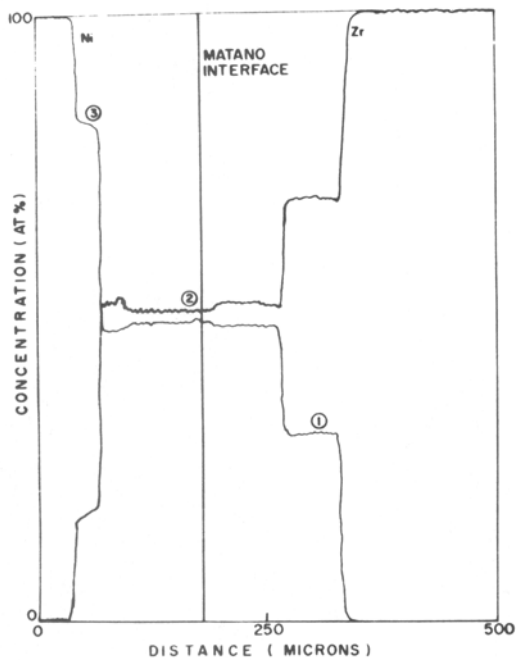
Fig. 9—Concentration penetration plots for the couple annealed at 1213 K for 144 h. The intermetallic compounds are marked as (1) NiZr$_2$, (2) NiZr, and (3) Ni$_5$Zr.

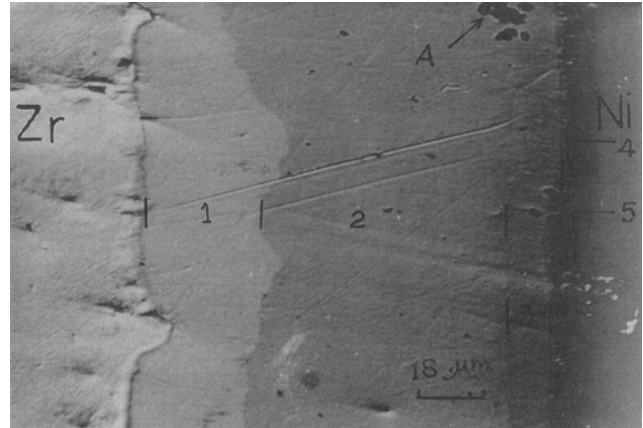| Compound	Temperature (K)	n	$K \times 10^{14}$ m^2/s
NiZr	1133	2.2	7.8
	1213	2.3	72.3
NiZr$_2$	1133	2.3	3.2
	1213	2.4	8.4
Ni$_{10}$Zr$_7$	1133	2.2	0.3
Ni$_5$Zr	1213	1.8	43.6

Fig. 10—Backscattered electron image of the couple annealed at 1169 K for 24 h. The presence of the markers (marked by "A") can be seen at the nickel side in the micrograph. The intermetallic compounds are marked as (1) NiZr$_2$, (2) NiZr, (3) Ni$_{10}$Zr$_7$, (4) Ni$_7$Zr$_2$, and (5) Ni$_5$Zr.

the diffusion zone cause the variation of the composition of the phases to a level to be detected by microanalytical techniques.

C. Diffusion Coefficients and Their Temperature Dependence

The diffusion coefficients have been evaluated both by Boltzmann-Matano-Heumann and Wagner methods and are listed in Table IV. Diffusion coefficients evaluated by these methods are reasonably comparable. A small discrepancy in the $\tilde{D}$ values is not unexpected, as there is a basic difference in the definition of $\tilde{D}$ and the method of its evaluation. The activation energy, $\tilde{Q}$, and the frequency factor, $\tilde{D}_0$, values have been obtained from the slope and the intercept in the plot of log $\tilde{D}$ as a function of the reciprocal of absolute temperature, $1/T$, using least

mean square analysis. These plots have been shown in Figure 11. The Arrhenius relationship thus established from these plots can well be represented by the following expressions:

$$\tilde{D}_{NiZr} = 2.26 \times 10^{-7}$$
$$\cdot \exp\left[(-119.0 \pm 13.4)/RT)\right] \quad \text{m}^2/\text{s}$$

$$\tilde{D}_{NiZr_2} = 1.2 \times 10^{-8}$$
$$\cdot \exp\left[(-103.0 \pm 25.0)/RT)\right] \quad \text{m}^2/\text{s}$$

Table I. Formation/Growth and Temperature Dependence of Various Intermetallic Compounds in the Diffusion Zone

Time (h)	Temperature (K)	Phase Thickness (μm)				
		Ni$_5$Zr	Ni$_7$Zr$_2$	Ni$_{10}$Zr$_7$	NiZr	NiZr$_2$
1	1133	1	2	2	9	7
7	1133	2	3	3	23	9
	1213	5	—	—	58	13
18	1133	2	3	7	53	19
	1213	5	—	—	91	25
24	1046	2	3	7	23	17
	1115	2	3	7	57	23
	1133	2	3	7	63	24
	1169	2	3	7	68	25
	1213	8	—	—	114	45
144	1213	23	—	—	200	63
237	1133	8	4	17	141	51
334	1213	35	—	—	325	70
459	1133	9	17	43	167	120

Table III. Composition of Various Phases in Zirconium/Nickel System

Phases	Composition of Zirconium (Atomic Fraction)		
	Nominal	At Phase Interface	At Diffusion Zone
Ni_5Zr	0.17	0.15 to 0.19	0.16 to 0.19
Ni_7Zr_2	0.22	0.22	0.22 to 0.23
$Ni_{10}Zr_7$	0.41	0.40 to 0.43	0.41 to 0.43
$NiZr$	0.50	0.50	0.49 to 0.50
$NiZr_2$	0.67	0.67	0.67 to 0.68

where T is temperature of annealing and R is expressed in kJ/mole.

D. Intermetallic Compounds in Diffusion Zone

Diffusion reaction between two metals leads, in principle, to the formation of all of the compounds, as depicted in the equilibrium phase diagram. In fact, all of the single-phase regions intersected by the isotherm, i.e., the temperature of the diffusion anneal, should appear in the diffusion zone in the same sequence as depicted in the phase diagram. In practice, because of nonequilibrium conditions prevailing in the diffusion zone, it is observed that only some or none of these phases appear in the diffusion zone.[18,19,20] Sometimes even metastable phases appear in the diffusion zone.[21] It is also observed that phases formed at lower temperature may disappear at higher temperatures.[22] Several excellent theoretical treatments describing the equilibrium state and the formation of intermetallic compounds in the diffusion zone have been published,[23–28] and many empirical models[29] have been suggested.

The formation of a new phase as a result of diffusion reaction between the parent phase is associated with net free energy change resulting from two competing processes. Whereas the formation of ordered intermetallics causes the lowering of free energy, the strain, vacancy supersaturation, and creation of new interfaces result in increase in free energy during the diffusion reaction. The nucleation of a phase is governed by their relative contributions to the net free energy change. Kale et al.[30] have discussed the criteria to rationalize it in terms of lattice mismatch between the nucleating phase and the parent phase. In addition to the thermodynamic aspects,
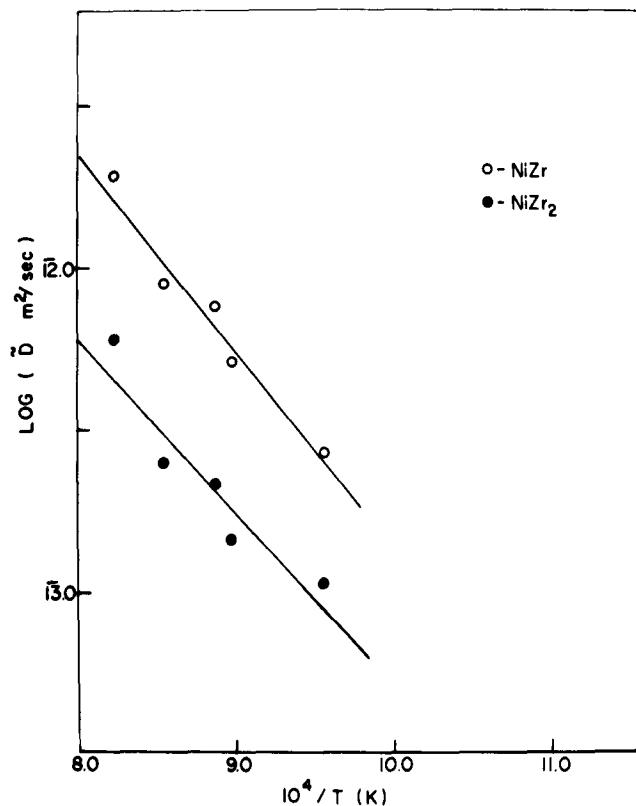

Fig. 11—Plots of $\log \bar{D}$ vs $1/T$ for NiZr and NiZr$_2$ compounds.

the growth of the intermetallic phase is controlled by the kinetics of the diffusion process, that is, the flux of atom species across the intermediate phase interface.

In the zirconium-nickel system, two intermetallic compounds, namely, Ni$_3$Zr and Ni$_{21}$Zr$_8$, do not nucleate out of seven possible intermediate phases in the temperature regime of the present studies. The absence of the intermetallic phase Ni$_{21}$Zr$_8$ is attributed to the fact that triclinic structure of this compound causes a large lattice mismatch with the parent matrix. The order of appearance and the growth of various compounds is predominantly governed by their respective diffusivities. Diffusivity values for the various intermetallic compounds are listed in Table IV. It can be seen that $\bar{D}_{NiZr} > \bar{D}_{NiZr_2} > \bar{D}_{Ni_{10}Zr_7} > \bar{D}_{Ni_7Zr_2} > \bar{D}_{Ni_5Zr}$, which is in accordance with the growth and the order of appearance in the diffusion zone (Figure 2). The phase Ni$_3$Zr does not

Table IV. Temperature Dependence of Interdiffusion Coefficients for Various Intermetallic Compounds

Temperature (K)	Method	Interdiffusion Coefficients $\bar{D} \times 10^{13}$ m^2/s				
		Ni_5Zr	Ni_7Zr_2	$Ni_{10}Zr_7$	$NiZr$	$NiZr_2$
1046	Boltzmann	0.02	0.06	0.25	2.68	1.08
	Wagner				1.40	0.81
1115	Boltzmann	0.04	0.10	0.38	5.18	1.43
	Wagner				6.41	1.93
1133	Boltzmann	0.06	0.14	0.42	7.60	2.19
	Wagner				7.94	2.16
1169	Boltzmann	0.07	0.15	0.43	8.90	2.50
	Wagner				9.19	2.39
1213	Boltzmann	—	—	—	19.00	6.00
	Wagner				24.60	7.03

Table V. Diffusivity Ratios of Intermetallics Disappearing at Higher Temperatures

Temperature (K)	Phases			
	Ni_7Zr_2		$Ni_{10}Zr_7$	
	$\tilde{D}_{Ni_7Zr_2}/\tilde{D}_{Ni_5Zr}$	$\tilde{D}_{Ni_7Zr_2}/\tilde{D}_{Ni_{10}Zr_7}$	$\tilde{D}_{Ni_{10}Zr_7}/\tilde{D}_{Ni_7Zr_2}$	$\tilde{D}_{Ni_{10}Zr_7}/\tilde{D}_{NiZr}$
1046	3.00	0.24	4.17	0.09
1115	2.50	0.26	3.85	0.07
1133	2.33	0.33	3.03	0.06
1169	2.14	0.35	2.86	0.05

appear at all in the diffusion zone, probably because it forms as a result of a peritectoid reaction and is expected to have very low diffusivity.

The stability of a phase depends upon its diffusivity with respect to that of adjoining phases.[31] The formation of a phase takes place if its transformation to another adjacent phase is less favorable than *vice versa*. Thus, the ratio of diffusivity values of a favorable phase with respect to the adjoining phase(s) should be more than unity. Consequently, the disappearance of a phase at higher temperature requires that the diffusivity ratios must decrease with increasing temperature. In the present case, it is observed that two phases, namely, Ni_7Zr_2 and $Ni_{10}Zr_7$, disappear at higher temperature (>1213 K). Table V lists various diffusivity ratios at different temperatures. It could be seen that formation of $Ni_{10}Zr_7$ is not favored with respect to phase NiZr. Thus, NiZr is expected to grow at the expense of $Ni_{10}Zr_7$. Similarly, Ni_7Zr_2 phase is expected to disappear at higher temperatures in favor of Ni_5Zr.

IV. CONCLUSIONS

1. The intermetallic compounds, namely, Ni_5Zr, NiZr, and $NiZr_2$, form in the diffusion zone at all temperatures between 1046 and 1213 K. The growth of these phases is found to be in the decreasing order of their diffusivities.
2. The compounds Ni_7Zr_2 and $Ni_{10}Zr_7$ disappear at higher temperatures. This is attributed to the relatively higher diffusivities of the adjacent phases.
3. The reaction index, n, for all compounds is nearly equal to 2, suggesting volume diffusion to be the main controlling diffusion process.
4. The appearance of Kinkendall voids and the markers on the nickel-rich side indicates the vacancy diffusion mechanism to be operative.
5. The activation energy values for interdiffusion in NiZr and $NiZr_2$ compounds are estimated to be 119.0 kJ/mole and 103.0 kJ/mole, respectively.

ACKNOWLEDGMENTS

REFERENCES

1. W.A. Ferrando: *Adv. Mater. Manufacturing Processes*, 1988, vol. 3 (2), pp. 195-231.
2. P. Nish and C.S. Jayanth: *Bull. Alloy Phase Diagrams*, 1984, vol. 5, pp. 144-48.
3. F.H. Hammad and H.I. Shaaban: *J. Nucl. Mater.*, 1979, vol. 80, pp. 152-58.
4. W.J. Meng, C.W. Lieh, E. Ma, B. Fultz, and W.L. Johnson: *Mater. Sci. Eng.*, 1988, vol. 97, pp. 87-91.
5. G.B. Kale: Ph.D. Thesis, University of Bombay, Bombay, India, 1987.
6. P.G. Shewmon: *Diffusion in Solids*, McGraw-Hill, New York, NY, 1960, p. 30.
7. Th. Heumann: *Z. Phys. Chem.*, 1952, vol. 201, pp. 16-20.
8. C. Wagner: *Acta Metall.*, 1969, vol. 17, pp. 99-107.
9. Gillaume F. Bastin and Frans. J.J. Van Loo: *Z. Metallkd.*, 1978, vol. Bd 69 (H8), pp. 540-45.
10. Johanns Maas, Guillaume F. Bastin, Frans J. Van Loo, and Ruday Metselaar: *Z. Metallkd.*, 1984, vol. Bd 75 (H2), pp. 140-45.
11. L.S. Castleman and L.L. Seigle: *Trans. TMS-AIME*, 1958, vol. 218, pp. 389-92.
12. S.B. NewComb and K.N. Tu: *Appl. Phys. Lett.*, 1986, vol. 48, pp. 1436-38.
13. A.D. Romig, Jr.: *Bull. Alloy Phase Diagrams*, 1987, vol. 8, pp. 308-22.
14. J.S. Kirkaldy: *Can. J. Phys.*, 1958, vol. 36, pp. 917-25.
15. J.W. Cahn and F. Larche: *Acta Metall.*, 1982, vol. 30, pp. 51-56.
16. P.W. Voorhees and W.C. Johnson: *J. Chem. Phys.*, 1986, vol. 84 (9), pp. 5108-21.
17. A.D. Romig, Jr. and J.I. Goldstein: *Metall. Trans. A*, 1983, vol. 14A, pp. 1224-27.
18. R.S. Timsit: *Acta Metall.*, 1985, vol. 33, pp. 97-104.
19. K. Hirano and Y. Iijima: *Diffusion in Solids—Recent Developments*, Detroit, MI, Sept. 17, 1984, TMS-AIME, Warrendale, PA.
20. K. Hirano and Y. Ipposhi: *J. Jpn. Inst. Met.*, 1986, vol. 32, pp. 815-20.
21. D.S. Williams, R.A. Rapp, and J.P. Hirth: *Metall. Trans. A*, 1981, vol. 12A, pp. 639-52.
22. R.V. Patil, G.B. Kale, and S.K. Khera: *J. Nucl. Mater.*, 1981, vol. 97, pp. 192-202.
23. J.S. Langer and R.F. Sekerka: *Acta Metall.*, 1976, vol. 24, pp. 1071-78.
24. A.J. Hickl and R.W. Heckel: *Metall. Trans. A*, 1975, vol. 6A, pp. 431-40.
25. S.R. Shatyanski, J.P. Hirth, and R.A. Rapp: *Acta Metall.*, 1975, vol. 23, pp. 1225-37.
26. H. Schalizried: *Solid State Reactions*, Academic Press, New York, NY, 1974, p. 120.
27. V.I. Dybkov: *J. Mater. Sci.*, 1987, vol. 22, pp. 4233-39.
28. Guan-Xing Li and G.W. Powell: *Acta Metall.*, 1985, vol. 33, pp. 23-31.
29. R.W. Walser and R.W. Bene: *J. Vac. Sci. Technol.*, 1977, vol. 14, pp. 925-29.
30. G.B. Kale, S.K. Khera, and R.V. Patil: *Mater. Sci. Forum.*, 1985, vol. 3, pp. 319-24.
31. G.V. Kidson: *J. Nucl. Mater.*, 1961, vol. 3, pp. 21-29.